# Low-Temperature Hydrocracking of LDPE to Narrow-Distribution $C_3H_8$-$C_5H_{12}$ Alkanes over Precision-Impregnated Ni/HZSM-5*

Dang Zhilong[1], Wang Heng[1], Zhao Lingxiao[1], Xie Xiangyu[1], Mao Ning[1], Bai Xiaowei[1], Dai Zhenghua[1,2], Li Jian[1†]

(1. State Key Laboratory of Chemistry and Utilization of Carbon Based Energy Resources, Xinjiang University, Urumqi Xinjiang 830017, China; 2. Key Laboratory of Coal Gasification and Energy Chemical Engineering of Ministry of Education, East China University of Science and Technology, Shanghai 200237, China)

**Abstract**: In this work, a 5 wt.% Ni/HZSM-5 catalyst is prepared via precision impregnation and applied in the low-temperature hydrocracking of low-density polyethylene (LDPE), realizing the directional conversion of LDPE into narrow-distributed $C_3$ (propane)-$C_5$ (pentane) alkanes using a simple catalytic system. Experimental results show that the LDPE conversion reaches 99.0%, the $C_3$-$C_5$ yield is 85.4 wt.%, and the selectivity toward the target products exceeds 99.0%. The catalyst exhibits excellent stability with no obvious deactivation after 5 recycling runs. The catalyst preparation parameters and reaction conditions are experimentally optimized, and the optimal preparation protocol is determined: HZSM-5 with a Si/Al ratio of 25 is used as the support with a Ni loading of 5 wt.%, followed by calcination at 550 ℃ for 4 h and reduction in a hydrogen atmosphere at 450 ℃ for 4 h. Hydrogen radical regulation experiments using $C_6H_{14}$ and $CH_3OH$ as model compounds confirmed that the polymerization of methyl radicals ($CH_3\cdot$) contributed to the high selectivity, and hydrogen radicals ($H\cdot$) mainly promoted the formation of small-molecule intermediates and stabilized the formation of alkanes from intermediates with carbon chain lengths of 3-5. This catalytic mechanism is proven to be universal for both LDPE and polypropylene. This work provides an efficient non-noble metal catalytic system and theoretical support for the directional conversion of waste polyethylene.

**Key words**: LDPE; Ni/HZSM-5; hydrocracking; $C_3$-$C_5$ alkanes; waste plastic recycling; catalyst stability

**DOI**: 10.13568/j.cnki.651094.651316.2026.04.20.0001

**CLC Number**: TQ511.3 **Document Code**: A **Article ID**: 2096-7675(2026)05-0588-015

**引文格式**: 党志龙,王衡,赵凌霄,谢翔宇,毛宁,白小薇,代正华,李建. Ni/HZSM-5上LDPE低温加氢裂化制备窄分布$C_3H_8$~$C_5H_{12}$烷烃[J]. 新疆大学学报(自然科学版中英文),2026,43(5):588-602.

**英文引文格式**: Dang Zhilong, Wang Heng, Zhao Lingxiao, Xie Xiangyu, Mao Ning, Bai Xiaowei, Dai Zhenghua, Li Jian. Low-temperature hydrocracking of LDPE to narrow-distribution $C_3H_8$-$C_5H_{12}$ alkanes over precision-impregnated Ni/HZSM-5[J]. Journal of Xinjiang University(Natural Science Edition in Chinese and English),2026,43(5):588-602.

# Ni/HZSM-5上LDPE低温加氢裂化制备窄分布$C_3H_8$~$C_5H_{12}$烷烃

党志龙[1], 王 衡[1], 赵凌霄[1], 谢翔宇[1], 毛 宁[1], 白小薇[1], 代正华[1,2], 李 建[1]

(1. 新疆大学 碳基能源资源化学与利用国家重点实验室,新疆 乌鲁木齐 830017;
2. 华东理工大学 煤气化及能源化工教育部重点实验室,上海 200237)

**摘 要**: 本文通过精密浸渍法制备了Ni负载量为5 wt.%的Ni/HZSM-5催化剂,并应用于低密度聚乙烯(LDPE)的低温加氢裂化,利用简单的催化体系将LDPE定向转化为窄分布的$C_3$(丙烷)~$C_5$(戊烷)烷烃. 实验结果表明,LDPE的转化率

* **Received Date**: 2026-04-20; **Revised Date**: 2026-06-03; **Accepted Date**: 2026-06-05.

**Foundation Item:** The Key Research and Development Project of Xinjiang Uygur Autonomous Region "Technology development for high-quality component recovery from oily sludge and efficient utilization of residues" (2025B01011); National Natural Science Foundation of China "Research on the mechanism of self-heating and product regulation during pyrolysis reaction of Xinjiang cotton stalk biomass under low oxygen conditions" (52266016).

**Biography:** Dang Zhilong (2000—), male, master student, research field: catalytic hydrogenolysis of polyethylene, E-mail: 2502496521@qq.com.

† **Corresponding Author:** Li Jian (1991—), male, associate professor, research field: biological thermochemical conversion, E-mail: jianli2246@163.com.

高达99.0%，$C_3$~$C_5$的产率为85.4 wt.%，目标产物的选择性超过99.0%，且催化剂表现出优异的稳定性，在5次循环使用后无明显失活. 对催化剂的制备参数和反应条件进行了优化，确定了最佳制备方案：以Si/Al比25的HZSM-5为载体，Ni负载量为5 wt.%，随后在550 ℃下煅烧4 h，并在450 ℃的$H_2$气氛中还原4 h. 使用$C_6H_{14}$和$CH_3OH$作为模型化合物进行的H·调节实验证实，高选择性是由$CH_3$·的聚合引起的，H·促进了小分子中间体的形成，并促进碳链长度为3~5的中间体稳定转化为烷烃. 实验表明该催化机制对LDPE和聚丙烯均适用. 本文提供了一种高效的非贵金属催化体系，并为废聚乙烯的定向转化提供了理论支持.

**关键词**：LDPE；Ni/HZSM-5；加氢裂化；$C_3$~$C_5$烷烃；废塑料再利用；催化剂稳定性

# 0 Introduction

Plastics are widely used due to their excellent chemical stability; however, their high resistance to degradation has led to the massive accumulation of waste plastics, emerging as a global environmental issue that needs urgent resolution[1]. Polyethylene (PE) and polypropylene (PP), as important polyolefin materials, account for a considerable proportion of global plastic output. At present, the recycling rate of waste polyolefins remains low, and most waste plastics end up in landfills or natural environments, causing severe ecological pollution and waste of carbon resources[2]. Chemical recycling technology can convert waste plastics into new chemical products, which not only alleviates environmental pressure but also realizes high-value recovery of carbon resources, making it a core solution strategy[3]. Hydrocracking has become a pivotal route for converting polyolefins into high-value petrochemical products owing to its high conversion rate and relatively low energy consumption[4].

The directional preparation of $C_3$-$C_5$ alkanes (liquefied petroleum gas-like (LPG) products) through the hydrocracking of low-density polyethylene (LDPE) has extremely high industrial application value due to its high product added value[5]. Converting waste LDPE into $C_3$-$C_5$ alkane feedstock for LPG can realize high-value utilization of plastic waste, supplement high-quality clean fuel sources, and reduce dependence on fossil-based LPG. Compared with traditional petroleum-derived routes, this path is more environmentally friendly, with lower carbon emissions and less pollution, and can fully leverage the advantages of LPG such as clean combustion, easy storage and transportation, good engine compatibility and high efficiency, so as to meet the dual needs of energy structure upgrading and plastic waste recycling[6].

Zeolite catalysts have attracted extensive attention in the field of polyolefin catalytic conversion because of their large specific surface area, strong acidity and outstanding thermal stability[7]. As a typical zeolite material, HZSM-5 has been widely applied in the hydrocracking of polyolefins[8], and its structural regulation and modification are the core approaches to improving catalytic selectivity. For instance, zeolites can be modified by alkali treatment, combined alkali-acid treatment, citric acid treatment and EDTA-2Na treatment[8]. Hierarchical single-crystal HZSM-5 zeolite (Hier-HZSM-5-*x*) synthesized with ordered mesoporous carbon-silicon composites as templates[9], mesoporous HZSM-5 prepared via post-synthesis modification and direct synthesis methods[10], HZSM-5/SiC foam structured catalysts[7], and HZSM-5 molecular sieves with extra-framework aluminum[11], all exhibit remarkable catalytic performance in the hydrocracking of polyethylene. It is proven that structural regulation and modification of HZSM-5 molecular sieves can significantly optimize the catalytic conversion performance of polyolefins. Nevertheless, the acid sites of pristine HZSM-5 possess low capability for hydrogen activation, which limits the cleavage of long-chain molecular segments. These modified molecular sieves suffer from high reaction temperature and low conversion efficiency in the hydrocracking of polyolefins.

Metal-based catalysts, serving as hydrogen activators, have been extensively investigated for polyolefin conversion. The Pt/$Nb_2O_5$ catalyst achieves a $C_5$-$C_{19}$ yield of 79.2 wt.% in the hydrocracking of polyethylene at 290 ℃[12]; The Pt/SZ catalyst displays a $C_5$-$C_{20}$ yield of 67.51 wt.% during LDPE cracking at 250 ℃[13]. The Ru/$CeO_2$ catalyst attains an LDPE conversion rate of 95% and a total yield of liquid fuels and waxy products of 82 wt.% at a low temperature of 280 ℃[14]; The Ru/HZSM-5 bifunctional catalyst delivers a polyethylene conversion rate of

82.53% and a $C_5$-$C_{21}$ yield of 62.87 wt.% under mild conditions[15]. It is evident that the introduction of metal active sites can effectively enhance product selectivity and catalytic efficiency in polyolefin conversion, and make the reaction conditions milder. Although noble metal catalysts exhibit excellent catalytic activity in hydrocracking reactions, their scarce reserves and high cost hinder large-scale industrial application, thereby rendering non-noble metal catalysts a current research hotspot[16].

Ni-based catalysts feature superior hydrogenation activity, favorable selectivity to gas-phase products and outstanding comprehensive catalytic performance, and are often combined with zeolite supports to construct bifunctional catalytic systems[17]. The Ni-WCE/HZSM-5 catalyst prepared by the impregnation method is applied to HDPE pyrolysis, achieving an oil yield of up to 80 wt.%[18]. The Ni-W/$ZrO_2$ bifunctional catalyst obtains a liquid fuel yield of 75.6 wt.% in polyolefin hydrocracking at 250 ℃[19]. When Co/HZSM-5 is used for pyrolysis and oil production from landfill waste plastics, the oil yield reaches 47.42 wt.%, and the high calorific value of products can reach 38.06 MJ/kg[20]. Although considerable research has been carried out on polyethylene depolymerization over non-noble metal catalysts, such catalytic systems generally show lower conversion efficiencies than noble metal counterparts with broad product distributions, which greatly increases the difficulty of subsequent separation and purification, especially for the fine separation of gas-phase products, and meanwhile require hydrogenolysis temperatures above 300 ℃ (up to 560 ℃) and reaction times longer than 8 h.

In this work, a 5 wt.% Ni/HZSM-5 bifunctional catalyst was fabricated via precision impregnation method, and its catalytic performance in the low-temperature hydrocracking of LDPE was systematically investigated. High raw material conversion was achieved under mild reaction conditions (280 ℃, 2 MPa $H_2$, 30 min), along with high-yield targeted production of $C_3$-$C_5$ alkanes with a product yield of 85.4 wt.% and selectivity exceeding 99.0%. Combined with the extremely low methane generation in experiments and verification results of model compound tests, a hypothetical reaction pathway of "depolymerization-polymerization-hydrogenation" for polyolefins within the pore channels of Ni/HZSM-5 was proposed. Model compound experiments were further conducted to corroborate the reaction mechanism.

# 1 Experimental Section

## 1.1 Materials

Powdered LDPE and PP were purchased from Sinopec Group, with a particle size of 200 mesh. HZSM-5 zeolite (provided by Nankai University Catalyst Factory) had a $SiO_2/Al_2O_3$ molar ratio of 25.0 (Table 1), possesses two types of elliptical pore structures. $Ni(NO_3)_2·6H_2O$ was of analytical grade, supplied by Tianjin Fengchuan Chemical Reagent Technology Co., Ltd.. All chemicals were used without further purification.

**Table 1 The basic characterization of HZSM-5**

| Molecular sieve | HZSM-5(NKF-5D-25HWH) |
|---|---|
| Appearance | White powder |
| $SiO_2/Al_2O_3$/(mol/mol) | 25.0 |
| Crystallinity/% | 96.0 |
| BET/($m^2$/g) | 348.0 |
| $Na_2O$/(m/m%) | 0.05 |
| LOI/(m/m%) | 9 |

## 1.2 Catalyst Preparation

A measured amount of nickel nitrate hexahydrate was dissolved in deionized water, and HZSM-5 zeolite was added. The mixture was stirred at 400 r/min for 4 h, evaporated to dryness at 70 ℃, dried overnight, and heated to 550 ℃ at 5 ℃/min in a muffle furnace for calcination (4 h). Before use, the catalyst was reduced in $H_2$ at 450 ℃

for 4 h in a reduction tube, with temperature programmed to rise at 5 ℃/min. The catalyst prepared by this method was denoted as p-Ni/HZSM-5 (precision impregnation), and the conventional impregnation sample was denoted as c-Ni/HZSM-5 for comparison. The relevant characterization of Ni/HZSM-5 is shown in Figure 1[21].

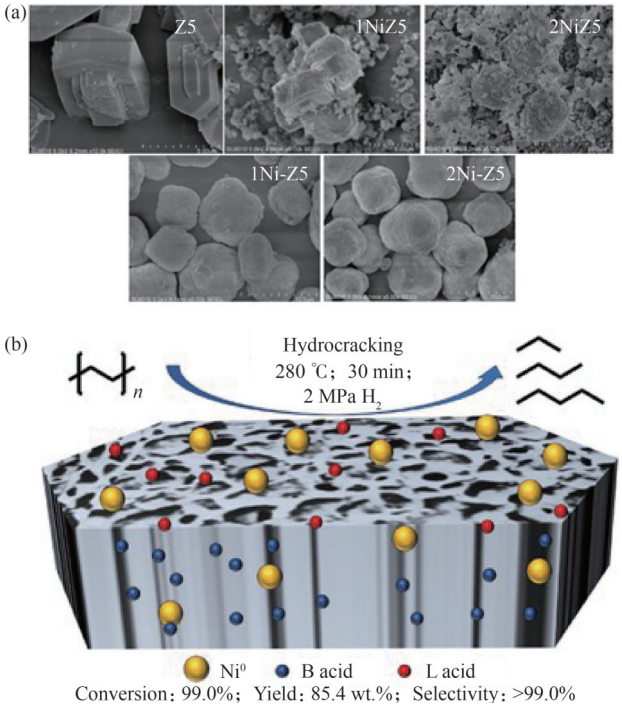



**Figure 1 (a) SEM of Ni-modified HZSM-5 zeolites; (b) Schematic of the structure when Ni is uniformly impregnated on HZSM-5**

### 1.3 Hydrocracking Experiment

LDPE hydrocracking was carried out in a 100 mL high-pressure reactor. 1.0 g of feedstock and 0.25 g of catalyst were loaded into the reactor. The reactor was purged with $H_2$ three times at 2 MPa, and finally pressurized to 2 MPa with $H_2$. The reactor was heated on a hot plate to 260 ℃-320 ℃, and the reaction time was recorded. After reaction, the reactor was cooled to room temperature. Gaseous products were collected in gas bags, identified qualitatively by GC-FID, and quantified based on the total volume calculated from the pressure after cooling. Soluble substances in the autoclave were extracted with dichloromethane, and characterized qualitatively and quantitatively by GC-MS and GC-FID. The remaining solids (catalyst and unreacted feedstock) were dried at 50 ℃ and weighed. All experiments were repeated three times to ensure accuracy, and the average values were reported.

### 1.4 Analytical Techniques

After cooling the autoclave, the pressure gauge reading was recorded. The gas volume under standard conditions was calculated using Formula (1). The gas in the autoclave was collected, and the composition and content of non-condensable gaseous products were quantified by gas chromatography equipped with a flame ionization detector and a thermal conductivity detector (GC-FID/TCD, SHIMADZU GC-2010). The mass of each gaseous component was calculated according to Formula (2):

$$pV = p_{\text{gas}} V_{\text{r}}, \tag{1}$$

$$M_{\text{gas}} = \frac{V \times \sum_{i=1}^{5} (\rho_i \times C_i)}{100}, \tag{2}$$

where $p$ is standard pressure (MPa); $V$ is gas product volume (mL); $p_{\text{gas}}$ is gas product pressure (MPa); $V_{\text{r}}$ is autoclave volume (mL); $M_{\text{gas}}$ is total mass of gas products (g); $\rho_i$ is density of alkanes with different carbon numbers

(g/cm$^3$); $C_i$ is volume fraction of component $i$ (%).

Gas components were quantified using an external standard calibration curve established with a standard gas mixture of known concentrations. The concentration of each component was calculated from the peak area measured by GC combined with the calibration curve, and the mass of each gas component was then converted according to Formula (2). Taking propane as an example, its calibration curve and fitting formula are shown in Figure 2.

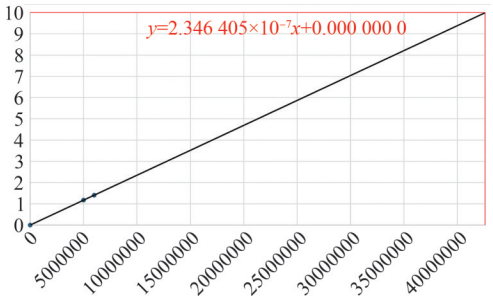



**Figure 2 Calibration curve of propane gas**

Note: The calibration curve formula for propane is $y = 2.346\,405\times10^{-7}x + 0.000\,000\,0$

The composition of liquid oil was analyzed by gas chromatography-mass spectrometry (GC-MS, PerkinElmer Clarus 690). The temperature program was set as follows: The initial temperature was maintained at 40 ℃ for 3 min, then increased to 280 ℃ at a rate of 10 ℃/min and held for 15 min, with a total running time of 42 min. The MS detection conditions were: Solvent delay time from 0 to 1.8 min, detection mode as MS Scan, scanning time from 1.80 to 42.00 min, scanning range from 35.00 to 500.00 m/z, and scanning speed at 0.30 s. The components in the chromatogram were identified by comparing with the standard spectra in the NIST MS library and the reported liquid products in relevant literature.

Quantitative analysis of plastic hydrocracking oil products was performed by gas chromatography-flame ionization detector (GC-FID, SHIMADZU GC-2010 Plus). The gas chromatogram was equipped with an SH-1701 capillary column (30 m×0.25 mm×0.25 μm) and an FID detector. The specific test conditions were inlet temperature: 280 ℃; detector temperature: 280 ℃; hydrogen flow rate: 40 mL/min; air flow rate: 400 mL/min; makeup gas flow rate: 30 mL/min; split ratio: 116∶1. The column oven temperature was kept at 40 ℃ for 3 min, then raised to 280 ℃ at a rate of 10 ℃/min and maintained for 15 min.

For the quantitative analysis of plastic hydrocracking liquid products by GC-FID (SHIMADZU GC-2010 Plus), the internal standard method (effective carbon number method) was applied, with dichloromethane as the solvent and cyclohexane as the internal standard.

The mass calculation formula of a single liquid product component is as follows:

$$m_i = \frac{ECN_s \times A_i \times m_s \times M_i}{ECN_i \times A_s \times M_s}, \tag{3}$$

where $ECN_s$ is effective carbon number of internal standard; $ECN_i$ is effective carbon number of the component to be detected; $A_s$ is FID response area of internal standard; $A_i$ is response area of the component to be detected; $m_s$ is mass of internal standard (g); $m_i$ is mass of the component to be detected (g); $M_s$ is molecular mass of internal standard (g/mol); $M_i$ is molecular mass of the component to be detected (g/mol).

In this study, quantitative calculations were performed using the following formulas based on gas chromatography detection results and gravimetric data, and all data were the average values of three parallel experiments.

1) Feedstock conversion:

$$X = \frac{m_0 - m_1}{m_0} \times 100\%, \tag{4}$$

where $X$ is feedstock conversion (%); $m_0$ is initial mass of feedstock before reaction (g); $m_1$ is mass of unreacted

feedstock after reaction (g).

2) Gas-phase product yield:

$$Y_g = \frac{m_g}{m_0} \times 100\%, \tag{5}$$

$$Y_{g1} = \frac{Y_g \times m_{g1}}{100} \times 100\%, \tag{6}$$

$$Y_{g2} = \frac{Y_g \times m_{g2}}{100} \times 100\%, \tag{7}$$

where $Y_g$ is total yield of gas-phase products (wt.%); $m_g$ is total mass of gas-phase products (g); $m_0$ is initial mass of feedstock before reaction (g); $Y_{g1}$ is yield of $C_1$-$C_2$ components (wt.%); $m_{g1}$ is area percentage of $C_1$-$C_2$ components; $Y_{g2}$ is yield of $C_3$-$C_5$ components (wt.%); $m_{g2}$ is area percentage of $C_3$-$C_5$ components.

3) Liquid-phase product yield:

$$Y_l = \frac{m_l}{m_0} \times 100\%, \tag{8}$$

where $Y_l$ is total yield of liquid-phase products (wt.%); $m_l$ is total mass of liquid-phase products (g); $m_0$ is initial mass of feedstock before reaction (g).

4) Solid-phase product yield:

$$Y_s = \frac{m_s}{m_0} \times 100\%, \tag{9}$$

where $Y_s$ is solid-phase product yield (wt.%); $m_s$ is total mass of solid-phase products (g); $m_0$ is initial mass of feedstock before reaction (g).

5) Carbon balance:

$$C_b = \frac{m_{gc} + m_{lc} + m_{sc}}{m_{0c}} \times 100\%, \tag{10}$$

where $C_b$ is carbon balance (%); $m_{gc}$ is mass of carbon in gas-phase products (g); $m_{lc}$ is mass of carbon in liquid-phase products (g); $m_{sc}$ is mass of carbon in solid-phase products (g); $m_{0c}$ is mass of carbon in initial feedstock before reaction (g).

6) Mass balance:

$$M_b = \frac{m_g + m_l + m_s}{m_0} \times 100\%, \tag{11}$$

where $M_b$ is mass balance (%); $m_g$ is total mass of gas-phase products (g); $m_l$ is total mass of liquid-phase products (g); $m_s$ is total mass of solid-phase products (g); $m_0$ is initial mass of feedstock before reaction (g).

7) $C_3$-$C_5$ selectivity:

$$S_{C3\text{-}C5} = \frac{m_{C3} + m_{C4} + m_{C5}}{m_g} \times 100\%, \tag{12}$$

where $S_{C3\text{-}C5}$ is selectivity of $C_3$-$C_5$ components (%); $m_{C3}$ is mass of propane (g); $m_{C4}$ is mass of *n*-butane and isobutane (g); $m_{C5}$ is mass of *n*-pentane and isopentane (g); $m_g$ is total mass of gas-phase products (g).

## 2 Results and Discussion

### 2.1 Product Distribution and Core Performance Analysis

Figure 3(a) is a schematic of the LDPE hydrocracking process, intuitively showing the conversion of LDPE into gas, liquid, and solid products under catalyst action. Combined with experimental data, gas yield reached 86.3 wt.%, $C_3$-$C_5$ selectivity exceeded 99.0%, solid product was only 0.8 wt.%, and liquid product was 3.0 wt.%, confirming efficient directional conversion of LDPE into gaseous $C_3$-$C_5$ products. The extremely low solid by-product yield indicates that the catalyst has excellent anti-coking performance, which is beneficial to the long-term operation of the reaction system.

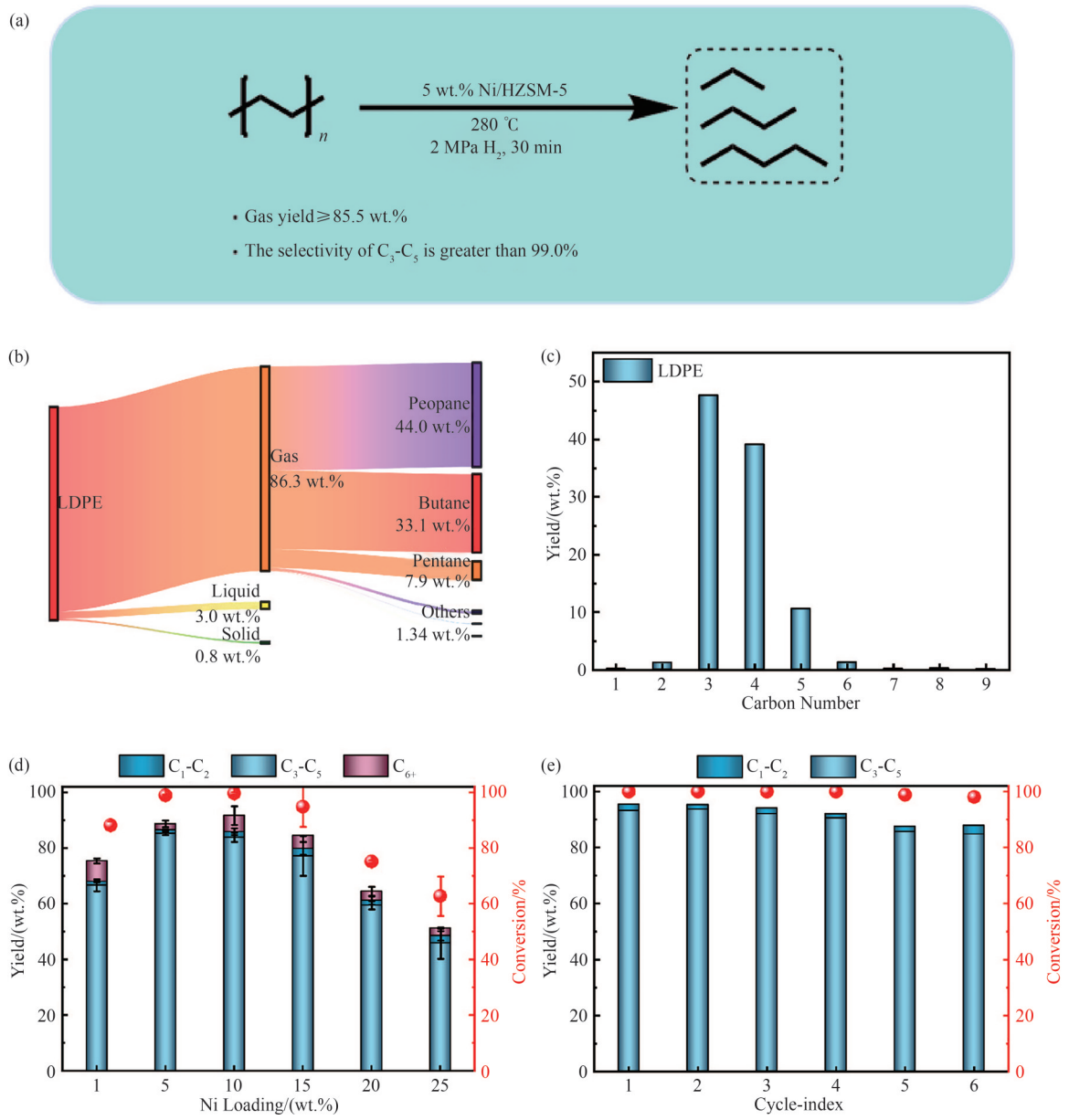



**Figure 3 Product distribution of LDPE (a) Hydrocracking process of LDPE; (b) Sankey diagram of LDPE products; (c) Carbon number distribution of LDPE products; (d) Effect of Ni loading; (e) Catalyst stability**

Figure 3(b) is a Sankey diagram showing product composition, with propane accounting for the highest proportion (44.0 wt.%), followed by butane (33.1 wt.%), pentane (7.9 wt.%), and liquid components (3.0 wt.%), further verifying high $C_3$-$C_5$ selectivity. Figure 3(c) is the product carbon number distribution, quantitatively showing that products were mainly $C_3$-$C_5$ light alkanes, with extremely low high-carbon products ($C_{6+}$), consistent with the Sankey diagram.

Figure 3(d) investigates the effect of Ni loading. With Ni loading increasing from 1 wt.% to 5 wt.%, LDPE conversion gradually increased and stabilized, and $C_3$-$C_5$ selectivity remained high. At 5 wt.% loading, both conversion and selectivity reached optimal values. This is because appropriate Ni loading increases metallic hydrogenation active sites, forming more synergistic centers with support acidic sites; excessive loading causes Ni grain aggregation, reducing active site dispersion and affecting catalytic performance. Thus, 5 wt.% was the optimal Ni loading, which balances the number of metal hydrogenation sites and acid cracking sites to realize the maximum synergistic effect.

Figure 3(e) shows catalyst stability test results. With the number of cycles increasing from 1 to 5, LDPE conversion and $C_3$-$C_5$ yield did not decrease significantly, indicating good structural stability and reusability. The excellent cyclic stability, combined with ultra-low solid by-product yield, supports the industrial application potential of the catalyst.

Table 2 compares the performance of the Ni/HZSM-5 catalyst prepared in this study with other Ni-loaded catalytic systems. It can be seen that the performance of this catalyst is significantly superior compared to those in other literature. The conversion rate of the raw materials is at a relatively high level, balancing high selectivity and high conversion rate. The selectivity of the target product reaches the ultimate level, and the directionality is far beyond the levels reported in the literature. The selectivity of $C_3$-$C_5$ alkanes is as high as 99.0%, effectively solving the drawback of low selectivity in other catalytic systems.

**Table 2 Comparison of catalytic performance between the Ni/HZSM-5 catalyst and other Ni-based catalysts**

| Catalyst | Reactant | Conversion/% | Selectivity of the target product/% | Liquid yield/(wt.%) | Gas yield/(wt.%) | Reference |
|---|---|---|---|---|---|---|
| Ni/H$\beta$ | HDPE | 94.0 | – | 78.6 | 15.2 | [17] |
| Ni-WCE/HZSM-5 | HDPE | 95.4 | $C_6$-$C_8$: 30.0 | 80.0 | – | [18] |
| Ni-W/$ZrO_2$ | LDPE | 94.0 | $C_5$-$C_{20}$: 85.6 | 75.6 | – | [19] |
| Ni/$SiO_2$ | LDPE | 96.0 | $C_6$-$C_{35}$: 76.0 | 65.0 | 20.0 | [22] |
| Ni/HZSM-5 | HDPE | 86.0 | Xylene: 27.3 | 64.8 | – | [23] |
| Ni/HZSM-5 | PC | 99.3 | $C_{15}$: 80.0 | 81.2 | – | [24] |
| Ni/HZSM-5 | LDPE | 99.0 | $C_3$-$C_5$: 99.0 | 3.0 | 86.3 | Ours |

## 2.2 Optimization of Catalyst Preparation Parameters and Performance Evaluation

In this study, the screening of suitable catalyst supports was first conducted. By loading nickel (Ni) onto different supports and molecular sieves and comparing their catalytic performance in the hydrogenolysis of LDPE, HZSM-5 has been confirmed as the best support material as shown in Figure 4.

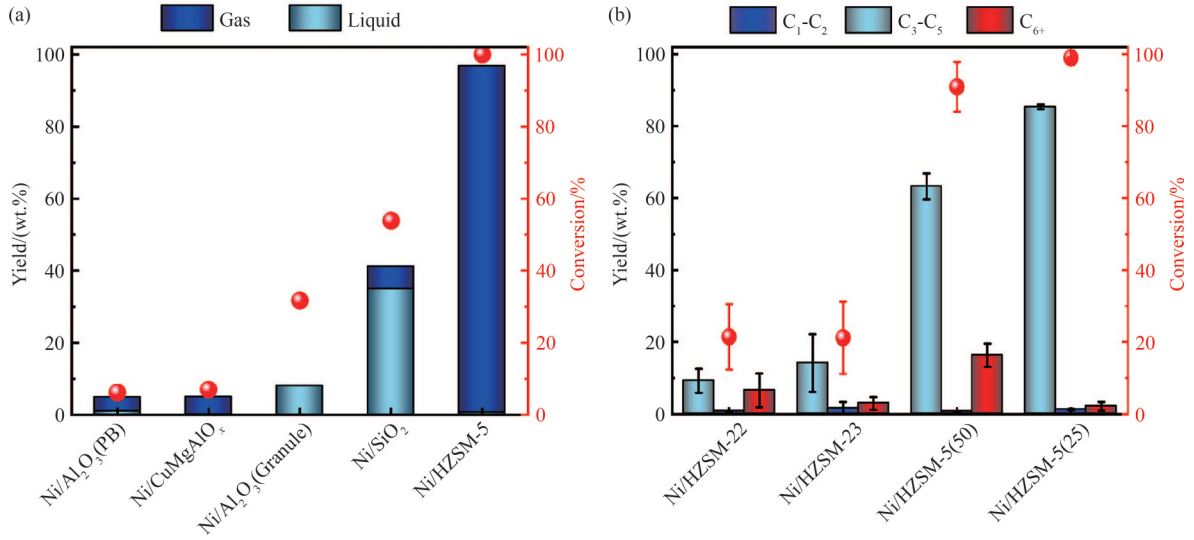



**Figure 4 Performance of Ni supported on (a) different supports and (b) different zeolites**

Table 3 presents the effects of different zeolite supports (HZSM-22, HZSM-23, HZSM-5), Si/Al ratios, and preparation methods (p-Ni/HZSM-5: precision impregnation; c-Ni/HZSM-5: conventional impregnation) on LDPE hydrocracking performance, with reaction conditions fixed at 280 ℃, 2 MPa $H_2$, and 30 min.

**Table 3 Hydrocracking of LDPE over different zeolites and preparation methods (280 ℃, 2 MPa $H_2$, 30 min)**

| Catalyst | Si/Al | Conversion/% | $C_3$-$C_5$ yield/(wt.%) | Mass balance/% |
|---|---|---|---|---|
| Ni/HZSM-22 | 25 | 21.5 | 9.3 | 96.0 |
| Ni/HZSM-23 | 25 | 21.2 | 14.2 | 98.0 |
| Ni/HZSM-5 | 50 | 90.9 | 63.3 | 91.6 |
| c-Ni/HZSM-5a | 25 | 95.5 | 74.2 | 93.4 |
| p-Ni/HZSM-5b | 25 | 99.0 | 85.4 | 91.8 |

Note: a denotes conventional impregnation; b denotes precision impregnation

As shown in Table 3, the support type exerts a significant effect on catalytic performance. The Ni-based catalysts supported on HZSM-22 and HZSM-23 exhibit low LDPE conversion of 21.5% and 21.2%, as well as low $C_3$-$C_5$ alkane yields of 9.3 wt.% and 14.2 wt.%. This is attributed to their one-dimensional pore structure, which imposes severe diffusion limitations on the depolymerized products of long-chain polyethylene. Meanwhile, the uneven distribution of acid sites makes it difficult to directionally produce light alkanes.

In comparison, HZSM-5-supported catalysts with a three-dimensional pore structure possess superior catalytic activity. Ni/HZSM-5 with a Si/Al ratio of 50 achieves an LDPE conversion of 90.9% and a $C_3$-$C_5$ alkane yield of 63.3 wt.%, confirming that the three-dimensional pore system of HZSM-5 alleviates diffusion limitation and its acid sites facilitate the cracking of long-chain hydrocarbons. Further comparison indicates that Ni/HZSM-5 with a Si/Al ratio of 25 shows better catalytic activity than the counterpart with a Si/Al ratio of 50. HZSM-5 with a lower Si/Al ratio contains more Brønsted acid sites, suggesting that Brønsted acid sites play a dominant role in the hydrocracking process.

The p-Ni/HZSM-5 (precision impregnation) had the best performance: 99.0% LDPE conversion, 85.4 wt.% $C_3$-$C_5$ yield, 86.3 wt.% gas yield, and 3.0 wt.% liquid yield. c-Ni/HZSM-5 (conventional impregnation) had slightly lower performance, because precision impregnation enables Ni active components to enter pores more easily, forming more effective metal-acid site pairs, strengthening hydrogenation-cracking synergy, and improving conversion efficiency and $C_3$-$C_5$ selectivity. Meanwhile, lower Si/Al ratio (25) increases support acidic site density, further promoting long-chain hydrocarbon cracking.

Table 4 investigates the effects of calcination and reduction temperatures on the performance of 5 wt.% Ni/HZSM-5. The catalyst without calcination and reduction exhibited extremely low activity (conversion: 30.4%, $C_3$-$C_5$ yield: 16.5 wt.%), since nickel existed in the form of nickel nitrate precursor without metallic Ni hydrogenation sites. The sample calcined at 550 ℃ but without reduction achieved 60.9% conversion and 51.9 wt.% $C_3$-$C_5$ yield. The absence of hydrogenation activity of NiO limited the hydrocracking performance.

**Table 4 Hydrocracking of LDPE over 5 wt.% Ni/HZSM-5 (Si/Al = 25) prepared by precision impregnation method under different calcination and reduction temperatures (280 ℃, 2 MPa $H_2$, 30 min)**

| Calcination temperature/℃ | Reduction temperature/℃ | Conversion/% | $C_3$-$C_5$ yield/(wt.%) | Mass balance/% |
|---|---|---|---|---|
| – | – | 30.4 | 16.5 | 91.4 |
| 550 | – | 60.9 | 51.9 | 95.9 |
| 550 | 350 | 94.1 | 75.1 | 89.5 |
| 550 | 400 | 91.7 | 72.4 | 92.5 |
| 550 | 450 | 99.0 | 85.4 | 91.8 |

Note: The symbol "–" represents the blank control group without undergoing calcination or reduction treatment

After calcination at 550 ℃ and reduction at different temperatures, catalytic performance improved significantly. With reduction temperature increasing from 350 ℃ to 450 ℃, LDPE conversion increased from 94.1% to 99.0%, $C_3$-$C_5$ yield increased from 75.1 wt.% to 85.4 wt.%, liquid yield decreased from 4.2 wt.% to 2.2 wt.%, and gas yield remained 74.0 wt.%-86.6 wt.%. This is because higher reduction temperature promotes complete reduction

of NiO to metallic $Ni^0$ active sites, improves Ni dispersion on the support, and regulates grain growth, forming more synergistic active centers with acidic sites, strengthening hydrocracking and directional generation of $C_3$-$C_5$ alkanes. The optimal condition was calcination at 550 ℃ and reduction at 450 ℃, consistent with p-Ni/HZSM-5 performance in Table 4, verifying rationality of catalyst preparation parameters.

### 2.3 Effects of Reaction Conditions on Hydrocracking Performance

Figure 5(a) shows the effect of reaction temperature. With temperature increasing from 260 ℃ to 300 ℃, LDPE conversion increased from 60% to 100%, $C_3$-$C_5$ yield increased significantly, and $C_1$-$C_2$ light hydrocarbons and $C_{6+}$ yields were low. Higher temperature provides sufficient thermal energy to overcome the activation barrier, accelerates long-chain polyethylene cleavage and depolymerization, and promotes synergy between acidic site-catalyzed cracking and Ni site-catalyzed hydrogenation, directionally generating $C_3$-$C_5$ products. By comparing the boiling point curves of pure LDPE and the LDPE-catalyst mixture system, it can be seen that the addition of the catalyst significantly reduced the initial evaporation temperature of LDPE (Figure 6(a)). However, excessively high temperature causes over-cracking (more $C_1$-$C_2$), so 280 ℃ was suitable (complete conversion and high $C_3$-$C_5$ selectivity).

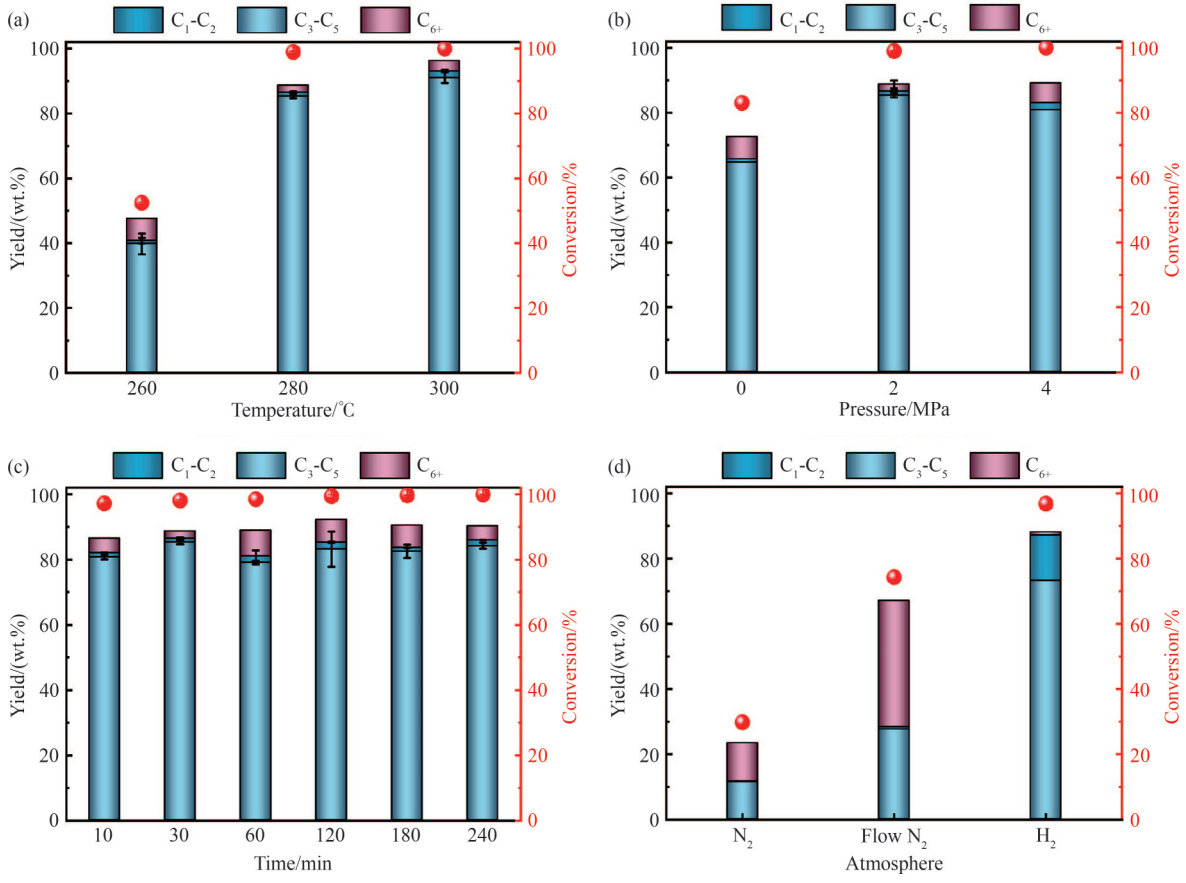



**Figure 5 Effects of reaction conditions on LDPE hydrocracking characteristics (a) Reaction temperature; (b) Hydrogen pressure; (c) Reaction time; (d) Different reaction atmospheres**

Figure 5(b) shows the effect of hydrogen pressure. In 0-2 MPa, LDPE conversion and $C_3$-$C_5$ yield increased significantly with pressure, and stabilized at 2 MPa. As a hydrogenation reagent, $H_2$ timely hydrogenates cracked unsaturated hydrocarbons to alkanes, avoiding polymerization into high-carbon products; meanwhile, $H_2$ inhibits catalyst coking and maintains active site function. Insufficient pressure causes incomplete hydrogenation (polymerization by-products, low $C_3$-$C_5$ selectivity); excessive pressure increases equipment cost without performance improvement. Thus, 2 MPa was optimal.

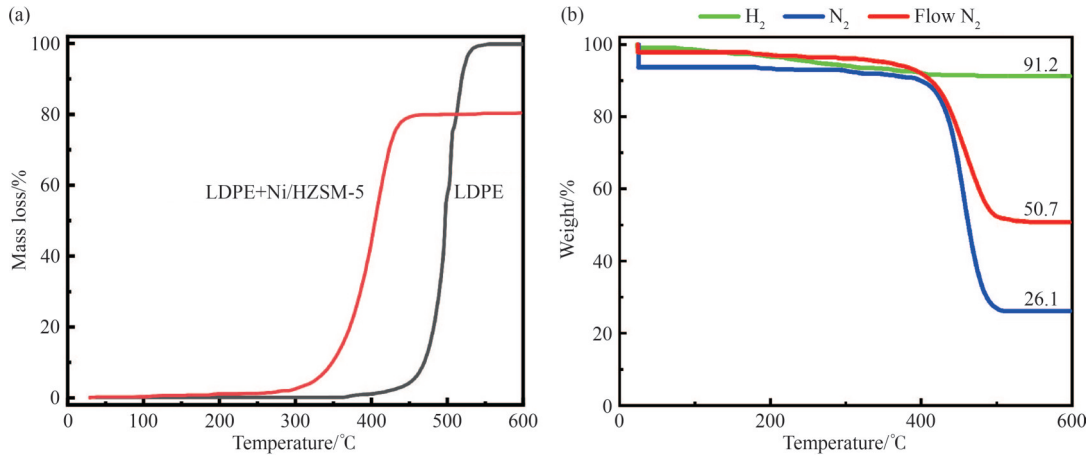



**Figure 6 (a) The boiling point curves of pure LDPE and LDPE mixed with catalyst (4:1); (b) TG curves plot of the residual solids from LDPE after reaction in different atmospheres**

Figure 5(c) shows the effect of reaction time. In 0-30 min, LDPE conversion and $C_3$-$C_5$ yield increased rapidly (30 min: 99.0% conversion, 85.4 wt.% $C_3$-$C_5$ yield). Extending time to 240 min, conversion remained stable, but $C_3$-$C_5$ yield decreased slightly and $C_{6+}$ increased, because some $C_3$-$C_5$ products undergo secondary polymerization into high-carbon hydrocarbons. Thus, 30 min was suitable.

Figure 5(d) compares the effects of two reaction atmospheres $H_2$ and $N_2$: The LDPE conversion and $C_3$-$C_5$ yield under $H_2$ atmosphere are both significantly higher than those under $N_2$ atmosphere, while under $N_2$ atmosphere, not only is the proportion of $C_{6+}$ products higher, but the amount of residual solids is also much greater than that under $H_2$ atmosphere (Figure 6(b)). Without $H_2$, cracked unsaturated hydrocarbons cannot be saturated timely, leading to polymerization/cyclization (high-carbon products, coking), reducing conversion and $C_3$-$C_5$ selectivity. This confirms $H_2$ is necessary for high $C_3$-$C_5$ selectivity.

### 2.4 Model Compound Experiments and Reaction Mechanism Hypothesis

The depolymerization mechanism of polyolefins in HZSM-5 pores and product selectivity origin remain unclear. Based on extremely low methane ($CH_4$) content in experiments, a "depolymerization-polymerization-hydrogenation" pathway was proposed, and verified by model compound experiments (methanol, *n*-hexane), with results shown in Figure 7.

Figure 7(a) shows methanol product carbon number distribution under optimal LDPE hydrocracking conditions: Products were mainly $C_3$-$C_5$, consistent with LDPE hydrocracking. Figure 7(b) proposes the methanol to $C_3$-$C_5$ pathway: Methanol first decomposes into carbon-containing active intermediates (e.g., $-CH_2-$, $-CH_3$), which polymerize into $C_3$-$C_5$ unsaturated hydrocarbons, and are finally hydrogenated at Ni active sites into saturated alkanes[25]. The results confirm that the polymerization of small-molecule carbon-containing intermediates is the core step for the formation of $C_3$-$C_5$ alkanes.

Figure 7(c) shows *n*-hexane product distribution (mainly $C_3$-$C_5$), indicating long-chain alkanes can be directionally cracked into $C_3$-$C_5$ products over the catalyst. Figure 7(d) compares the theoretical reaction mechanism and experimentally proposed mechanism of *n*-hexane. Theoretically, long-chain alkanes are prone to random cracking to generate products with different carbon numbers[26], while in the experiment, the products were highly concentrated in the $C_3$-$C_5$ range. It is inferred that long-chain alkanes first undergo preliminary cleavage into small-molecule intermediates, which form $C_3$-$C_5$ unsaturated hydrocarbons via selective polymerization, and are finally hydrogenated to the target products[27]. Meanwhile, based on the experimental results of LDPE hydrogenolysis catalyzed by acidic pore-enlarged catalysts, pore enlargement treatment shows no significant effect on product yield and carbon number distribution. Therefore, it can be inferred from Figure 8 that pore size is not the primary factor responsible for the high selectivity toward $C_3$-$C_5$ compounds.

Figure 7(e) contrasts the differences between the traditional reaction pathway and the new one. The traditional reaction pathway mainly involves random cleavage of LDPE long-chain molecules, resulting in a wide product distribution and low selectivity. The new reaction pathway, after the cleavage of long-chain molecules, involves subsequent polymerization and hydrogenation, narrowing the product distribution to the $C_3$-$C_5$ range and effectively suppressing the formation of methane products.

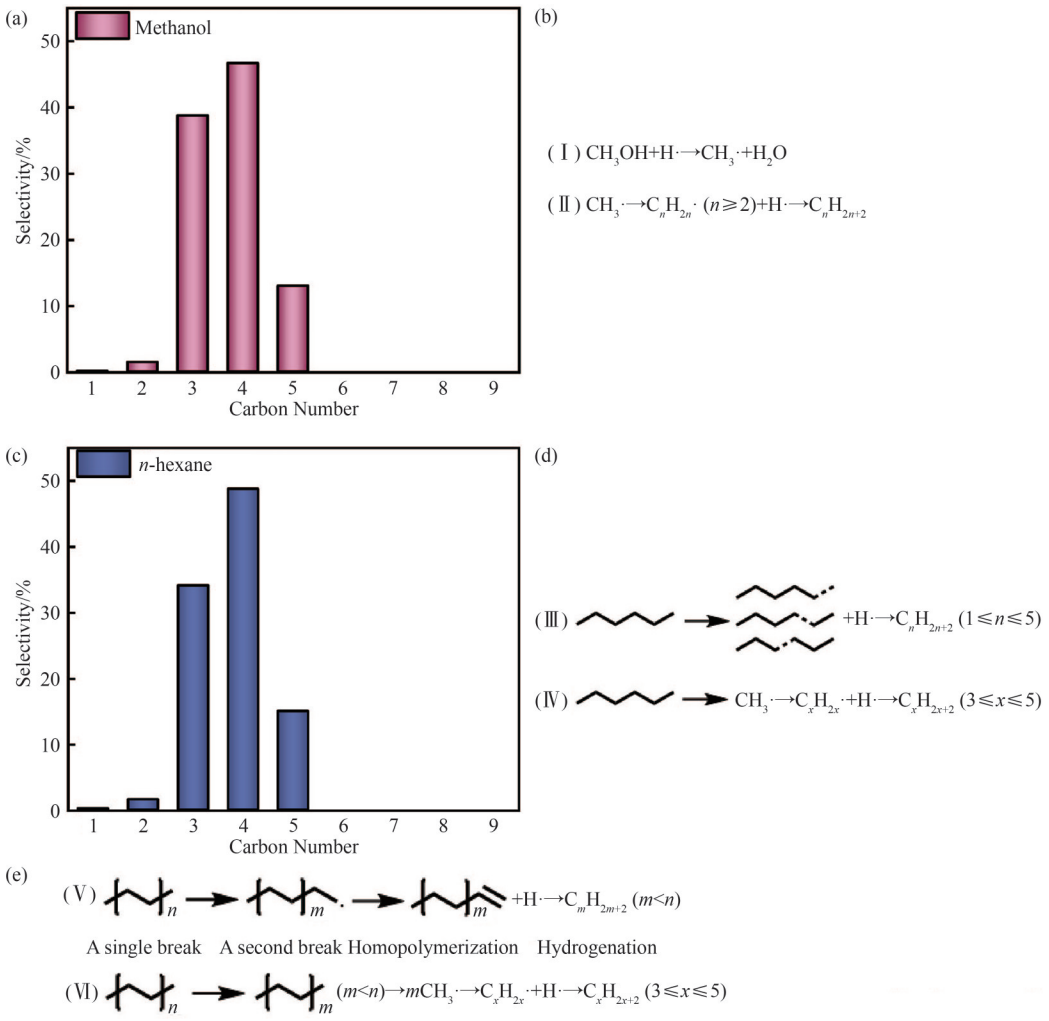



**Figure 7 Reaction pathways of model compounds (a) Product distribution of methanol under the optimal conditions for LDPE hydrocracking; (b) Pathways for the formation of $C_3$-$C_5$ products from methanol; (c) Product distribution of *n*-hexane under polyethylene hydrogenolysis reaction conditions; (d) Theoretical reaction mechanism and experimental reaction mechanism hypothesis of *n*-hexane; (e) Comparison between existing hydrocracking pathways and the proposed pathway**

## 2.5 Experimental Verification of Reaction Mechanism

Figure 9(a) and Figure 9(b) reveal the regulatory effect of hydrogen radical (H·) content on product distribution. High H· content increased $C_3$-$C_5$ selectivity (extremely low $C_1$-$C_2$); low H· content slightly increased $C_1$-$C_2$ and decreased $C_3$-$C_5$ selectivity. This is because H· promotes long-chain molecule depolymerization into small-molecule intermediates and inhibits overcracking, providing conditions for intermediate polymerization into $C_3$-$C_5$ hydrocarbons.

Figure 9(b) further shows that $H_2$ atmosphere and 2 MPa pressure increase H· concentration; $N_2$ atmosphere has extremely low H· content (low product selectivity), consistent with the hydrocracking performance under different atmospheres. We used methanol as raw material: $C_3$-$C_5$ selectivity under $H_2$ (appropriate pressure) was significantly higher than under $N_2$, and higher H· concentration increased $C_3$-$C_5$ selectivity, confirming the key role of H· in polymerization and supporting the mechanism hypothesis.

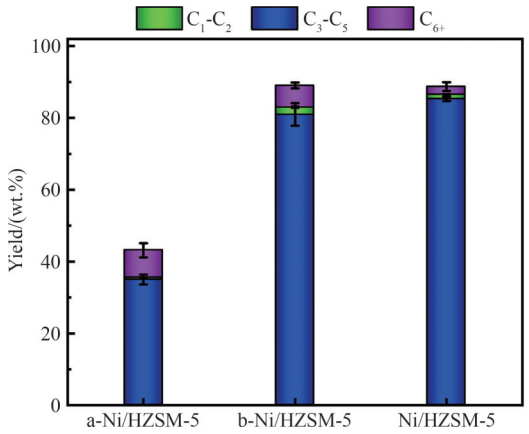



**Figure 8 The influence of acid-washed catalysts on the hydrogenolysis of LDPE**

Note: a-Ni/HZSM-5 was loaded first and then acid-washed; b-Ni/HZSM-5 was acid-washed first and then loaded

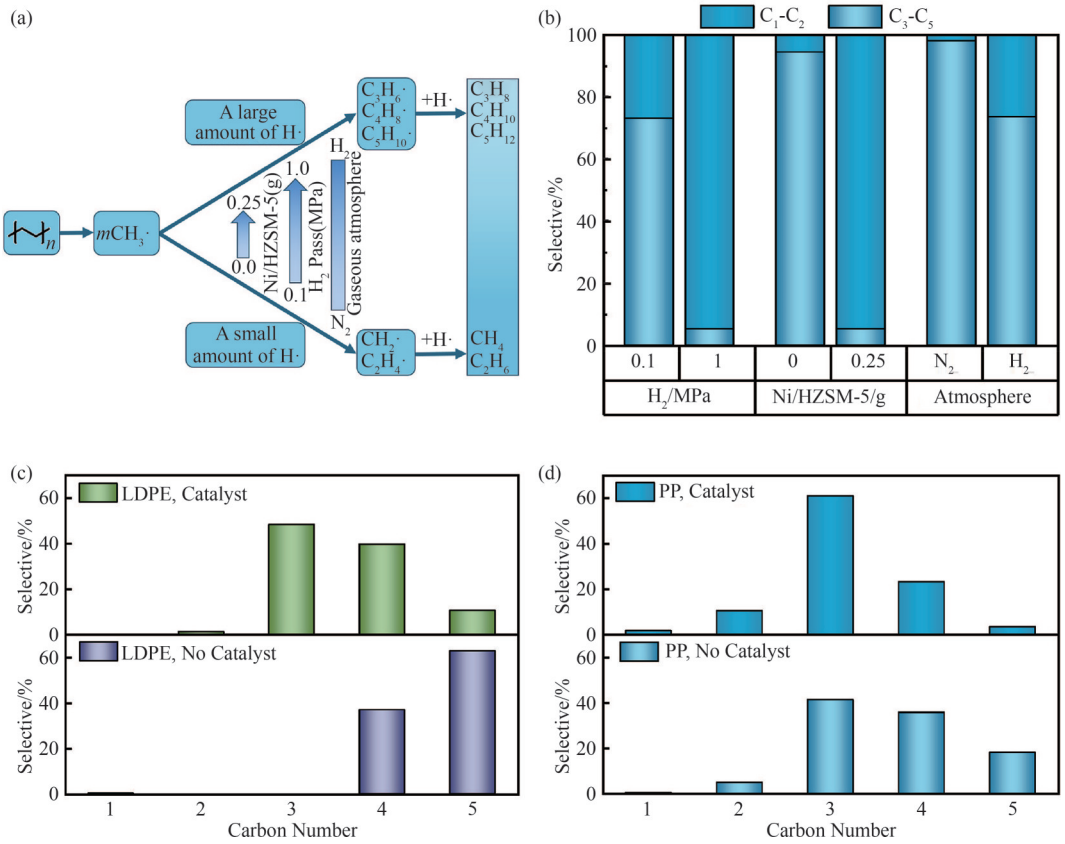



**Figure 9 Effect of hydrogen radical content on product distribution (a) Effects of different conditions on hydrogen radical concentration leading to changes in product distribution; (b) With methanol as raw material, changes in product selectivity of $C_1$-$C_2$ and $C_3$-$C_5$ under different reaction conditions; (c) Carbon number distribution of LDPE with and without catalyst; (d) Carbon number distribution of PP with and without catalyst**

Figure 9(c-d) compare LDPE/PP product distribution with and without catalyst: without catalyst, product distribution was wide (low $C_3$-$C_5$ selectivity, a high content of high-carbon products); with Ni/HZSM-5, products were highly concentrated in $C_3$-$C_5$ (high selectivity). This is because the synergistic effect of the metal-acid sites of the catalyst regulates the generation of hydrogen radicals (H·), promotes the polymerization and hydrogenation of intermediates, and as shown in Figure 10, this mechanism is still applicable in polypropylene, indicating its universality. This further verifies the rationality of the "depolymerization-polymerization-hydrogenation" reaction mechanism.

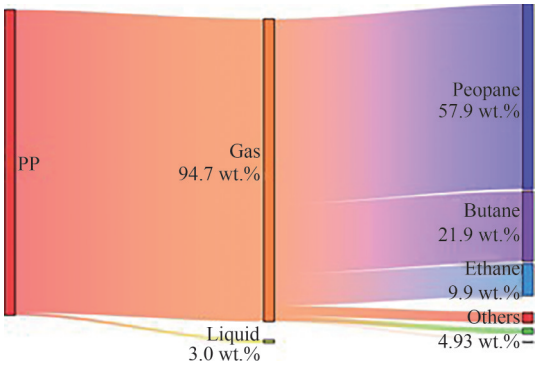



**Figure 10 Schematic of hydrocracking products from polypropylene**

## 3 Conclusions

To address the low recycling rate of waste polyethylene, high energy consumption, wide product distribution, difficult separation, and unclear polyolefin depolymerization mechanism in HZSM-5 pores, this study conducted LDPE hydrocracking experiments over Ni/HZSM-5, with main findings as follows.

This study compared the preparation conditions of the catalysts and screened out the most effective catalyst preparation scheme, which was loading 5 wt.% Ni on HZSM-5 (Si/Al = 25), followed by calcination at 550 ℃ for 4 h and reduction at 450 ℃ for 4 h. Under the reaction conditions of 280 ℃, 2 MPa $H_2$ and a reaction time of 30 min, this catalyst showed excellent catalytic performance for the hydrogenolysis of LDPE and extreme stability. The main products were narrow-distributed $C_3$-$C_5$ alkanes, with a selectivity as high as 99.0%. Moreover, through experiments with model compounds, a new reaction pathway, namely the "depolymerization-polymerization-hydrogenation" reaction pathway, was proposed and verified. This pathway can clearly explain the experimental phenomena of high selectivity and low methane yield. Additionally, experiments proved that this catalyst also had good catalytic performance for PP.

## References:

[1] Geyer R, Jambeck J R, Law K L. Production, use, and fate of all plastics ever made[J]. Science Advances, 2017, 3(7): e1700782.

[2] Sambyal P, Najmi P, Sharma D, et al. Plastic recycling: Challenges and opportunities[J]. The Canadian Journal of Chemical Engineering, 2025, 103(6): 2462-2498.

[3] Liu S B, Kots P A, Vance B C, et al. Plastic waste to fuels by hydrocracking at mild conditions[J]. Science Advances, 2021, 7(17): eabf8283.

[4] Sun J K, Dong J H, Gao L J, et al. Catalytic upcycling of polyolefins[J]. Chemical Reviews, 2024, 124(16): 9457-9579.

[5] Woo S, Baek S, Lee K. On-board LPG reforming system for an LPG · hydrogen mixed combustion engine[J]. International Journal of Hydrogen Energy, 2020, 45(21): 12203-12215.

[6] Ajuka L O, Kazeem R A, Kuti O A, et al. Decarbonized automotive fuel: Liquefied petroleum gas biosynthesis, benefits and drawbacks[J]. Results in Engineering, 2024, 21: 101889.

[7] Zhou N, Dai L L, Lyu Y C, et al. A structured catalyst of ZSM-5/SiC foam for chemical recycling of waste plastics via catalytic pyrolysis[J]. Chemical Engineering Journal, 2022, 440: 135836.

[8] Liu Z, Wen N, Huang X Y, et al. The catalytic pyrolysis performance of waste plastics enhanced by different modified zeolite molecular sieves[J]. Catalysis Letters, 2026, 156(2): 52.

[9] Hou Y X, Li X Y, Sun M H, et al. The effect of hierarchical single-crystal ZSM-5 zeolites with different Si/Al ratios on its pore structure and catalytic performance[J]. Frontiers of Chemical Science and Engineering, 2021, 15(2): 269-278.

[10] Paula T P, Marques M F V, da Costa-Marques M R. Influence of mesoporous structure ZSM-5 zeolite on the degradation of urban plastics waste[J]. Journal of Thermal Analysis and Calorimetry, 2019, 138(5): 3689-3699.

[11] He X Y, Tian Y J, Guo L H, et al. Fabrication of extra-framework Al in ZSM-5 to enhance light olefins production in catalytic cracking of *n*-pentane[J]. Journal of Analytical and Applied Pyrolysis, 2022, 165: 105550.

[12] Lu S L, Liu X H, Guo Y, et al. Efficient hydrocracking of waste polyethylene into branched liquid fuels over low Pt-loaded $Nb_2O_5$ catalyst[J]. ChemSusChem, 2025, 18(6): e202402042.

[13] Utami M, Wijaya K, Trisunaryanti W. Pt-promoted sulfated zirconia as catalyst for hydrocracking of LDPE plastic waste into liquid fuels[J]. Materials Chemistry and Physics, 2018, 213: 548-555.

[14] Nakaji Y, Tamura M, Miyaoka S, et al. Low-temperature catalytic upgrading of waste polyolefinic plastics into liquid fuels and waxes[J]. Applied Catalysis B: Environmental, 2021, 285: 119805.

[15] Gao L, Zhong X, Liu J, et al. Selective upcycling of polyethylene over Ru/H-ZSM-5 bifunctional catalyst into high-quality liquid fuel at mild conditions[J]. ChemSusChem, 2024, 17(19): e202400598.

[16] Zhan J H, Dai R H, Cong R F, et al. Upgrading of waste polyolefins with non-noble metal catalysts[J]. Green Chemistry, 2025, 27(13): 3398-3412.

[17] Zhang G Q, Mao Q G, Yue Y Q, et al. Ni-based catalysts supported on H$\beta$ zeolite for the hydrocracking of waste polyolefins[J]. RSC Advances, 2024, 14(23): 15856-15861.

[18] Mohamad-Dzol M A A, Balasundram V, Shameli K, et al. Catalytic pyrolysis of high-density polyethylene over nickel-waste chicken eggshell/HZSM-5[J]. Journal of Environmental Management, 2022, 324: 116392.

[19] Leng C H, Li H J, Zhou Q F, et al. Selective hydrocracking of polyolefin waste into branched liquid fuels over a non-noble metal bifunctional Ni-W/$ZrO_2$ catalyst[J]. Journal of Materials Chemistry A, 2025, 13(33): 27546-27556.

[20] Koti A, Khongprom P, Ratanawilai S. Catalytic pyrolysis oil from landfilled plastics through Ni/HZSM-5 and Co/HZSM-5 catalysts[J]. ACS Omega, 2025, 10(6): 5744-5755.

[21] Wei Q, Zhang P F, Liu X D, et al. Synthesis of Ni-modified ZSM-5 zeolites and their catalytic performance in *n*-octane hydroconversion[J]. Frontiers in Chemistry, 2020, 8: 586445.

[22] Vance B C, Kots P A, Wang C, et al. Ni/$SiO_2$ catalysts for polyolefin deconstruction via the divergent hydrogenolysis mechanism[J]. Applied Catalysis B: Environmental, 2023, 322: 122138.

[23] Pan Z Y, Xue X F, Zhang C S, et al. Production of aromatic hydrocarbons by hydro-liquefaction of high-density polyethylene (HDPE) over Ni/HZSM-5[J]. Journal of Analytical and Applied Pyrolysis, 2018, 136: 208-214.

[24] Liu J Y, Wei J D, Feng X, et al. Ni/HZSM-5 catalysts for hydrodeoxygenation of polycarbonate plastic wastes into cycloalkanes for sustainable aviation fuels[J]. Applied Catalysis B: Environmental, 2023, 338: 123050.

[25] Łukaszuk K A, Rojo-Gama D, Øien-Ødegaard S, et al. Zeolite morphology and catalyst performance: Conversion of methanol to hydrocarbons over offretite[J]. Catalysis Science & Technology, 2017, 7(22): 5435-5447.

[26] Mu C, Sun J H, Xie C, et al. Shape selectivity of AEL channels for anomalously facilitating biojet fuel production from long-chain *n*-alkane hydrocracking[J]. ACS Catalysis, 2024, 14(3): 1394-1404.

[27] Xi X, Yang Y, An H L, et al. Preparation of the Ru/HZSM-5 catalyst and its catalytic performance for the 2-pentanone hydrodeoxygenation reaction[J]. New Journal of Chemistry, 2021, 45(37): 17692-17698.

**责任编辑：刘　敏**